Journal of Molecular Spectroscopy 268 (2011) 211–220

Contents lists available at ScienceDirect

Journal of Molecular Spectroscopy

journal homepage: www.elsevier.com/locate/jms

Fourier transform synchrotron spectroscopy of torsional and CO-stretching bands of $CH_3{}^{17}OH$

G. Moruzzi [a], R.J. Murphy [b], J. Vos [b], R.M. Lees [c], A. Predoi-Cross [b,*], B.E. Billinghurst [d]

[a] Dipartimento di Fisica "Enrico Fermi" dell'Università di Pisa, Largo B. Pontecorvo 3, I-56127 Pisa, Italy
[b] University of Lethbridge, Department of Physics and Astronomy, 4401 University Drive, Lethbridge, Canada AB T1K 3M4
[c] Centre for Laser, Atomic and Molecular Sciences, Physics Department, University of New Brunswick, Saint John, Canada NB E2L 4L5
[d] Canadian Light Source, Inc., University of Saskatchewan, 101 Perimeter Drive, Saskatoon, Canada SK S7N 0X4

ARTICLE INFO

Article history:
Available online 31 May 2011

Keywords:
Methanol
Far-infrared spectra
Fourier transform spectra
Internal rotation
Ritz analysis
CO-stretching band
Perturbations

ABSTRACT

The Fourier transform spectrum of the $CH_3{}^{17}OH$ isotopologue of methanol has been recorded in the 65–1200 cm^{-1} spectral region at a resolution of 0.00096 cm^{-1} using synchrotron source radiation at the Canadian Light Source. Here we present an extension to higher torsional states of our investigation of the torsion–rotation transitions within the small-amplitude vibrational ground state, now including assignments of more than 16 500 lines involving quantum numbers in the ranges $v_t \leqslant 3$, $J \leqslant 30$ and $|K| \leqslant 12$, as well as a study of the strong CO-stretching band centered at 1020 cm^{-1}. Energy term values have been determined for assigned ground and CO-stretching levels by use of the Ritz program, and have been fitted to series expansions in powers of $J(J+1)$ to determine substate origins and effective B values. Several Fermi anharmonic and Coriolis level-crossing resonances coupling the CO stretch with high torsional ground-state levels have been identified and characterized. The study is motivated by astrophysical applications, with a principal aim being the compilation of an extensive set of energy term values to permit prediction of astronomically observable sub-millimetre transitions to within an uncertainty of a few MHz.

1. Introduction

The advent of powerful new infrared and submillimeter-wave telescopes entering new regimes of sensitivity, resolution and frequency coverage has brought a need, recognized by astronomers and spectroscopists alike [1], for vastly extended laboratory databases of molecular spectra in support of the astronomical observations. The increase in sensitivity of detection will be such that, in addition to the normal isotopic species, lines from many of the rarer isotopologues will also be visible, greatly multiplying requirements for new laboratory data. Methanol is one of the most abundant interstellar and protostellar molecules and is found throughout the universe in a wide variety of astronomical sources, motivating our study of the $CH_3{}^{17}OH$ isotopic species for which little previous information has been available [2,3].

In our first report on the far-infrared (FIR) synchrotron spectrum of $CH_3{}^{17}OH$ from 120 to 350 cm^{-1} [4], we presented assignments and power-series expansion coefficients for a substantial number of torsion–rotation substates in the vibrational ground state. The assigned sub-bands corresponded principally to $v_t = 1 \leftarrow 0$ and $2 \leftarrow 1$ transitions for K values up to 10, where v_t is the torsional quantum number and K is the component of rotational angular momentum along the near-symmetry a-axis of the molecule. In the present work, which includes the spectral regions from 65 to 120 and >350 cm^{-1}, we have substantially extended the assignments up to higher $v_t = 2$ and $v_t = 3$ torsional levels and higher values of K, and have also been able to assign low-frequency $\Delta v_t = 0$ rotational sub-bands. The latter now allow connections to be established among all of the energy substates for each of the A and E symmetry species, thereby reducing the number of independent families of states to just two. We have also moved upward in the spectrum to analyze the strong CO-stretching band centered around 1020 cm^{-1}. Assignments of this band can frequently be followed to higher values of the overall rotational quantum number J than in the ground state spectrum, so give valuable additional support and confirmation for the ground-state assignments through combination difference checks. Given the great current interest in exploring hot cores and protostellar star-forming regions in the giant interstellar clouds where gas densities and temperatures are high, it is likely that significant emission from relatively highly excited states will be observed, so that laboratory studies of both high torsional levels and low-lying vibrational states will be of importance.

In this paper, we present our further progress in sub-band assignments for FIR and IR spectra of $CH_3{}^{17}OH$ obtained on the

* Corresponding author. Fax: +1 403 329 2057.
E-mail address: Adriana.predoicross@uleth.ca (A. Predoi-Cross).

0022-2852/$ - see front matter © 2011 Elsevier Inc. All rights reserved.
doi:10.1016/j.jms.2011.05.007

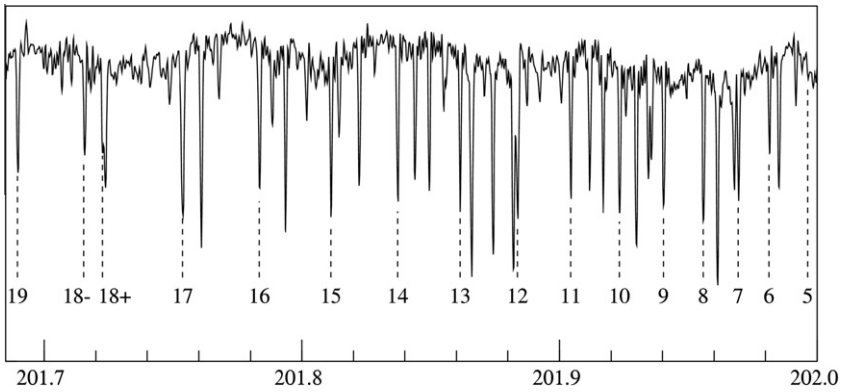

Fig. 1. Sample of the $CH_3{}^{17}OH$ FIR spectrum, showing the Q-branch of the $(v_t, K) = (3, 4) \leftarrow (3, 5)$ A sub-band. A localized level-crossing resonance splits the $J = 18$ line, perturbing the A^- component to lower wavenumber.

FIR beamline at the Canadian Light Source synchrotron facility, together with term value analysis carried out with the modified Ritz program [5,6]. In addition to v_t, K and J, we classify the energy levels [7] by the $A^{\pm}$ or E torsional symmetry σ and the small-amplitude vibrational state v. Both the vibrational ground state and the excited CO-stretching state are dealt with in the present work, and will be labeled as $v = gr$ and $v = co$, respectively. As before, our term values have been fitted to Taylor-series expansions in powers of $J(J + 1)$, in which the first three terms of the expansions correspond to substate origins, effective state-dependent B-values, and effective centrifugal distortion constants D, respectively. The latter also contain significant contributions from $\Delta K = \pm 1$ and ± 2 asymmetry coupling terms, so act as sensitive indicators of resonances arising from accidental near-degeneracies in the energy manifold.

Table 1
J-independent origins of assigned $CH_3{}^{17}OH$ sub-bands of A torsional symmetry. Uncertainties in the last quoted digit are shown in parentheses.

v'	v'_t	K'	v''	v''_t	K''	S	v_0 (cm^{-1})		o–c
gr	0	8	gr	0	7	A	53.1053	(28)	0.0160
gr	0	9	gr	0	8	A	67.7578	(16)	−0.0260
gr	0	10	gr	0	9	A	61.84	(28)	0.1185
gr	0	11	gr	0	10	A	65.15	(71)	0.1806
gr	0	12	gr	0	11	A	84.40094	(75)	0.0067
gr	1	0	gr	1	1	A	283.588650	(49)	0.0060
gr	1	0	gr	0	1	A	67.748190	(72)	0.0137
gr	1	1	gr	0	0	A	225.874620	(64)	−0.0029
gr	1	1	gr	0	2	A	199.752920	(48)	−0.0070
gr	1	2	gr	0	1	A	197.508210	(40)	−0.0008
gr	1	2	gr	0	3	A	172.820920	(71)	0.0047
gr	1	3	gr	0	2	A	248.666580	(71)	0.0158
gr	1	3	gr	1	4	A	218.756100	(62)	0.0096
gr	1	3	gr	0	2	A	67.245880	(83)	0.0159
gr	1	4	gr	0	3	A	299.51060	(13)	−0.0121
gr	1	4	gr	1	5	A	238.20759	(17)	−0.0273
gr	1	4	gr	0	3	A	59.444	(15)	−0.0324
gr	1	5	gr	0	4	A	236.66637	(26)	−0.0220
gr	1	5	gr	0	6	A	157.64427	(47)	−0.0095
gr	1	6	gr	0	5	A	229.54004	(18)	0.0074
gr	1	6	gr	0	7	A	154.80244	(34)	0.0271
gr	1	7	gr	0	6	A	302.224250	(72)	0.0193
gr	1	7	gr	1	8	A	213.41092	(15)	0.0060
gr	1	7	gr	0	6	A	111.70972	(26)	−0.0091
gr	1	8	gr	0	7	A	304.73231	(12)	−0.0322
gr	1	8	gr	1	9	A	183.8753	(12)	−0.0162
gr	1	8	gr	0	7	A	38.58	(14)	0.3052
gr	1	9	gr	0	8	A	252.55533	(16)	−0.0431
gr	1	9	gr	0	10	A	123.10993	(38)	0.0128
gr	1	10	gr	0	9	A	268.8930	(11)	0.0292
gr	1	10	gr	1	11	A	142.21501	(26)	0.0392
gr	1	10	gr	0	9	A	84.09405	(45)	0.0449
gr	1	11	gr	0	10	A	353.65415	(30)	−0.0309
gr	1	11	gr	1	12	A	204.26374	(82)	−0.0567
gr	1	11	gr	0	10	A	146.44991	(22)	−0.0889
gr	2	0	gr	1	1	A	342.574370	(52)	−0.0098
gr	2	0	gr	1	1	A	126.734030	(48)	−0.0019
gr	2	1	gr	0	0	A	473.104030	(56)	0.0024
gr	2	1	gr	1	0	A	179.481180	(48)	−0.0085
gr	2	1	gr	1	2	A	265.561720	(76)	−0.0016

Table 2
J-independent origins of assigned $CH_3{}^{17}OH$ sub-bands of E torsional symmetry. Uncertainties in the last quoted digit are shown in parentheses.

v'	v'_t	K'	v''	v''_t	K''	S	v_0/cm^{-1}		o–c
gr	0	−12	gr	0	−11	E	70.48678	(34)	0.0228
gr	0	−11	gr	0	−10	E	72.42786	(16)	−0.0390
gr	0	−10	gr	0	−9	E	74.53205	(13)	−0.0201
gr	0	−9	gr	0	−8	E	56.6825	(96)	0.0175
gr	1	−12	gr	0	−11	E	341.28067	(17)	0.0179
gr	1	−12	gr	1	−11	E	147.60891	(17)	−0.0520
gr	1	−11	gr	0	−12	E	133.18576	(24)	0.0479
gr	1	−11	gr	0	−10	E	266.10060	(34)	0.0319
gr	1	−11	gr	1	−10	E	71.83466	(37)	0.0363
gr	1	−10	gr	0	−11	E	121.83738	(36)	0.0339
gr	1	−10	gr	0	−9	E	268.79766	(13)	−0.0248
gr	1	−9	gr	0	−10	E	198.64076	(14)	−0.0687
gr	1	−9	gr	0	−8	E	329.85157	(11)	−0.0751
gr	1	−9	gr	1	−8	E	84.98730	(34)	−0.1070
gr	1	−8	gr	0	−9	E	188.18460	(13)	0.0173
gr	1	−8	gr	0	−7	E	287.795030	(92)	0.0237
gr	1	−8	gr	1	−7	E	104.96073	(15)	−0.0007
gr	1	−7	gr	0	−8	E	139.90293	(15)	0.0320
gr	1	−7	gr	0	−6	E	232.56178	(20)	−0.0004
gr	1	−6	gr	0	−7	E	162.155890	(87)	−0.0091
gr	1	−6	gr	0	−5	E	257.035990	(85)	−0.0284
gr	1	−5	gr	0	−6	E	247.54470	(26)	−0.0306
gr	1	−5	gr	0	−4	E	317.93961	(16)	−0.0135
gr	1	−5	gr	1	−4	E	97.807380	(88)	−0.0394
gr	1	−4	gr	0	−5	E	194.891260	(88)	0.0156
gr	1	−4	gr	0	−3	E	237.867950	(89)	0.0172
gr	1	−3	gr	0	−4	E	163.024420	(57)	0.0041
gr	1	−3	gr	0	−2	E	206.32298	(15)	−0.0047
gr	1	−2	gr	0	−3	E	209.694280	(63)	−0.0137
gr	1	−2	gr	0	−1	E	249.357560	(78)	−0.0064
gr	1	−1	gr	0	−2	E	268.55649	(10)	0.0044
gr	1	−1	gr	0	0	E	277.5270470	(83)	0.0086
gr	1	−1	gr	1	0	E	77.812150	(58)	0.0111
gr	1	0	gr	0	−1	E	204.844440	(64)	0.0330
gr	1	0	gr	0	1	E	194.214550	(63)	−0.0024
gr	1	1	gr	0	0	E	193.435290	(80)	0.0001
gr	1	1	gr	0	2	E	186.94466	(11)	0.0031
gr	1	2	gr	0	1	E	262.763510	(78)	0.0126
gr	1	2	gr	0	3	E	244.045180	(81)	0.0057
gr	1	3	gr	0	2	E	274.47309	(16)	−0.0109

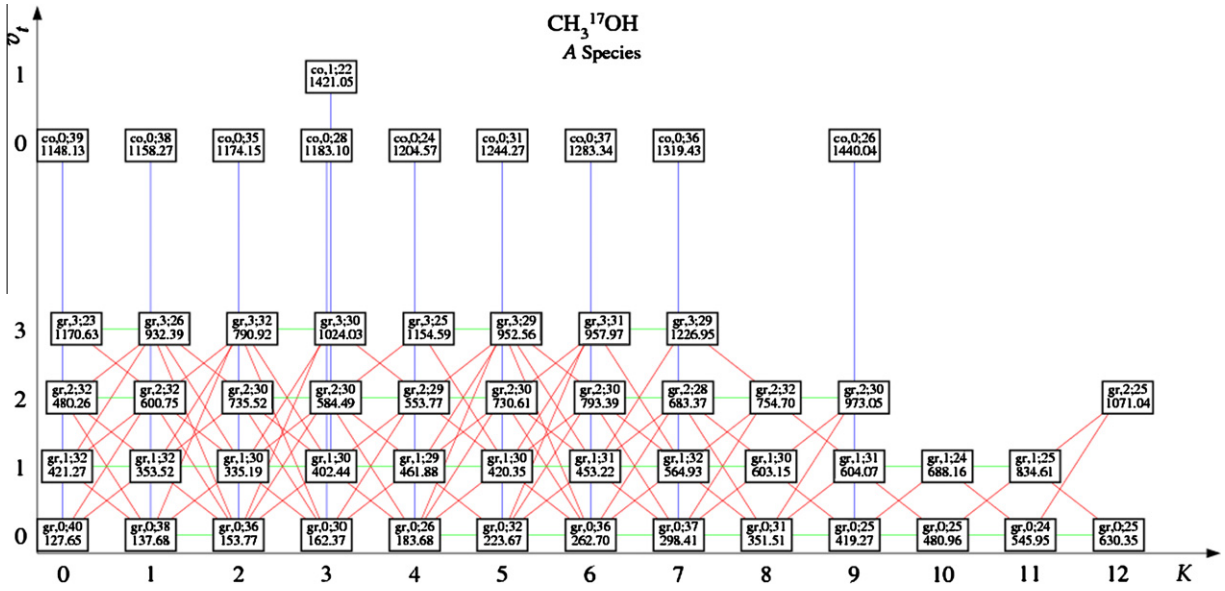

Fig. 2. Assigned substates of *A* torsional symmetry for $CH_3{}^{17}OH$. Substate boxes contain the vibrational state (gr = ground, co = CO stretch), the range of *J* for identified levels, and the *J*-independent origin of the substate. Assigned sub-bands are shown as lines connecting the boxes, with rotational $\Delta v_t = 0$ sub-bands indicated in green, $\Delta v_t > 0$ torsion–rotation sub-bands in red, and CO-stretching sub-bands in blue. (For interpretation of the references to color in this figure legend, the reader is referred to the web version of this article.)

For the CO-stretching band, we have modeled the origins with simple Fourier fits to the torsional energies, thereby clearly exposing the familiar strong $K = 0A$ and $-5E$ Fermi anharmonic resonances between the CO stretch and the ground-state $v_t = 3$ and $v_t = 4$ levels plus smaller Fermi shifts for the $-1E$, $4A$ and $6E$ substates [7–10]. We have also observed and characterized two interesting Coriolis level-crossing resonances coupling the CO stretch and $v_t = 3$ ground states. In order to derive effective molecular parameters characterizing the positions of the ground-state sub-bands, the sub-band origins were least-squares fitted to a torsion–*K*-rotation Hamiltonian. Our experimental measurements and results, including tables of assigned line positions, derived energy term values, Taylor-series expansion coefficients and asymmetry *K*-doubling parameters, have been deposited as Supplementary material.

2. Experimental

The $CH_3{}^{17}OH$ spectrum was recorded at the full resolution of 0.00096 cm^{-1} (1/MOPD) on the Bruker IFS125HR Fourier Transform spectrometer on the FIR beamline at the Canadian Light Source in Saskatoon. A pathlength of 12 m in a multipass cell was employed, with a pressure of 30 mTorr at room temperature. A total of 199 double scans were co-added. We attempted to

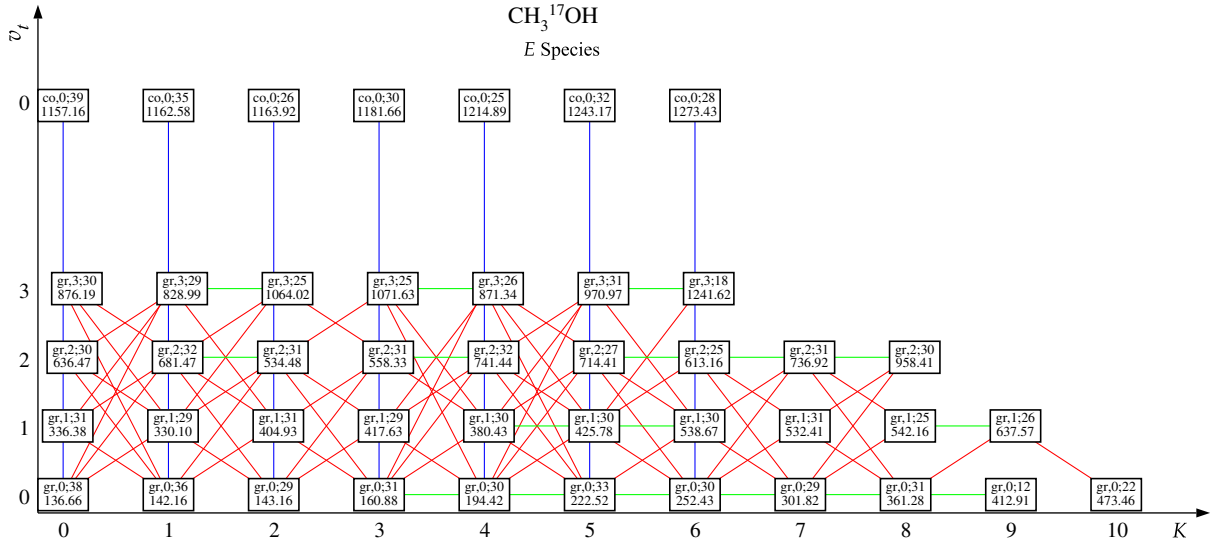

Fig. 3. Assigned substates of *E* torsional symmetry for $K \geqslant 0$ for $CH_3{}^{17}OH$. Substate boxes contain the vibrational state (gr = ground, co = CO stretch), the range of *J* for identified levels, and the *J*-independent origin of the substate. Assigned sub-bands are shown as lines connecting the boxes, with rotational $\Delta v_t = 0$ sub-bands indicated in green, $\Delta v_t > 0$ torsion–rotation sub-bands in red, and CO-stretching sub-bands in blue. (For interpretation of the references to color in this figure legend, the reader is referred to the web version of this article.)

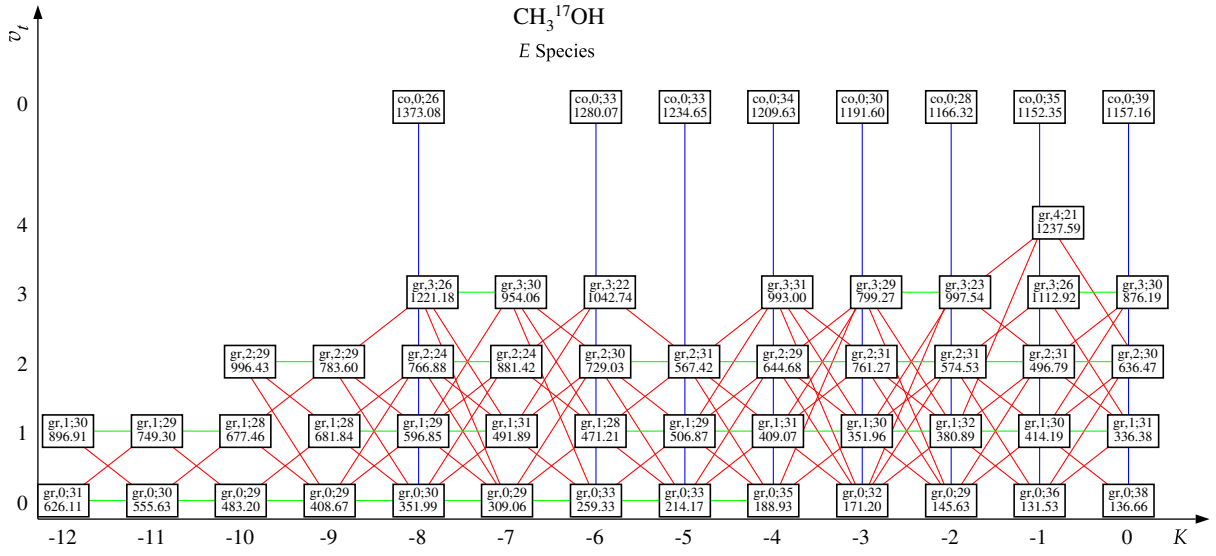

Fig. 4. Assigned substates of E torsional symmetry for $K \leqslant 0$ for $CH_3{}^{17}OH$. Substate boxes contain the vibrational state (gr = ground, co = CO stretch), the range of J for identified levels, and the J-independent origin of the substate. Assigned sub-bands are shown as lines connecting the boxes, with rotational $\Delta v_t = 0$ sub-bands indicated in green, $\Delta v_t > 0$ torsion–rotation sub-bands in red, and CO-stretching sub-bands in blue. (For interpretation of the references to color in this figure legend, the reader is referred to the web version of this article.)

remove the channels present in our spectra using one of the methods described in [11]. The sample was supplied by Merck, Sharpe and Dohme, with enrichment of 50% in ^{17}O. We found the bulk of the remaining 50% was the ^{18}O species with also a significant component of the normal ^{16}O species, so that the stronger lines from all three isotopologues were observable in the spectra. The spectra were calibrated using the line positions from [7] for the $CH_3{}^{16}OH$ transitions in the spectrum. Fig. 1 shows a sample of the spectrum containing the Q-branch of the $(v_t, K) = (3, 4) \leftarrow (3, 5)$ A sub-band, illustrating an interesting local resonance at $J = 18$ discussed later in Section 5 and demonstrating the high spectral resolution at the synchrotron. The $J = 18A^+$ line at 201.72259 cm^{-1} is separated by just 0.00098 cm^{-1} from the stronger line above it at 201.72357 cm^{-1}, yet is quite distinctly resolved. Similarly, the pair of lines at 201.935 cm^{-1}, separated by 0.00130 cm^{-1}, is well resolved.

3. Analysis with the Ritz program

In the Ritz program, all assigned transitions are fitted by least squares to a set of energy term values [5,6]. Since there can be many independent transitions connecting a given ground-state level to other levels with either the same or different v_t, the system is strongly over-determined and very reliable level energies can be derived. As discussed previously [4], the Ritz FIR assignments were achieved rapidly by interpolation between known lines of the $CH_3{}^{16}OH$ [7] and $CH_3{}^{18}OH$ [12] isotopologues via the scheme

$$\nu(^{17}O) = \frac{\nu(^{16}O) + \nu(^{18}O)}{2} + W\frac{\nu(^{16}O) - \nu(^{18}O)}{2} \quad (1)$$

where the adjustable interpolation parameter has a relatively constant value $W \approx -0.06$ for the ground state. For the CO-stretching band, on the other hand, the value of W varies markedly with K and J around the most common value of $W \approx -0.035$. This is likely associated with the fact that the CO-stretching band is qualitatively different for normal $^{12}CH_3{}^{16}OH$ with about twice the width for the J-multiplets in the P and R branches than is seen for $^{13}CH_3OH$, $CH_3{}^{18}OH$ and the present $CH_3{}^{17}OH$ species.

With lines from all three isotopologues present, the problem of line overlap and blending is acute, and numerous shoulders and anomalous widths are seen in the spectrum. Here, the profile fitting tool in the Ritz program [4] was extremely useful to disentangle blended profiles in order to extract reliable line positions and relative intensities, notably for the compact J-multiplets in the CO-stretching P and R branches.

We have now assigned 123 torsion–rotation sub-bands for the ground state in addition to those reported in the earlier work [4]. To illustrate their distribution throughout the spectrum, the sub-band origin wavenumbers are given in Tables 1 and 2 for A and E symmetries as determined from fitting to Taylor-series expansions in powers of $J(J + 1)$. The rms origin errors from the fits are shown in parentheses in Tables 1 and 2 and represent the uncertainties in the last quoted digit for the sub-band origins. Our current state of knowledge about the ground-state energy manifold is summarized pictorially in Figs. 2–4, where the boxes represent the identified substates connected by lines representing all of the assigned sub-bands. As can be seen, there are multiple links to most substate boxes, indicating that the energies of those states are well established by a variety of independent transitions. Table 3 shows a sample of the data set for the Ritz program illustrating the highly over-determined character of the observations for a representative set of levels. This large group of transitions accesses the $(v_t, K) = (3, 4)A$ ground levels for $J = 16$–20 in the neighborhood of the local resonance discussed below in Section 5, serving to fix the term values very accurately.

For the CO-stretching band, we have so far assigned 23 sub-bands in the $v_t = 0$ fundamental plus one in the $v_t = 1$ torsionally hot band, as shown in Figs. 2–4. The wavenumbers were again fitted to series expansions in powers of $J(J + 1)$ to determine the J-independent origins listed in Tables 1 and 2.

As illustrated in Table 3, all assigned transitions were input into the Ritz program to obtain term values for both ground and excited CO-stretching states. A sample of the output obtained is shown in Table 4, giving the term values obtained for the set of $(v_t, K) = (3, 4)A$ levels of Table 3 and also for the nearby $(0, 1)A$ CO-stretching levels involved in the level-crossing resonance. (Note that quadrupole splittings due to the ^{17}O nucleus are not re-

Table 3
Sample sets of $CH_3{}^{17}OH$ transitions accessing common upper levels, illustrating the form of the Ritz dataset, the high degree of over-determination of level positions within the energy manifold, and the comparison with wavenumbers calculated from the derived Ritz term values.

v'	v'_t	K'	J'	Sy'	v''	v''_t	K''	J''	Sy''	Obs. (cm^{-1})	Calc. (cm^{-1})	ε (cm^{-1})
gr	3	4	16	A	gr	1	5	16	A	733.47550	733.475545	2.00e−04
gr	3	4	16	A	gr	1	5	17	A	706.75870	706.75867	2.00e−04
gr	3	4	16	A	gr	2	3	15	A	594.63440	594.63438	2.00e−04
gr	3	4	16	A	gr	2	3	16	A	569.50230	569.50237	2.00e−04
gr	3	4	16	A	gr	3	5	15	A	226.87340	226.87335	2.00e−04
gr	3	4	16	A	gr	3	5	16	A	201.78340	201.78348	2.00e−04
gr	3	4	16	A	gr	3	5	17	A	175.12900	175.12901	2.00e−04
gr	3	4	17	A	gr	1	5	16	A	760.10019	760.10025	2.00e−04
gr	3	4	17	A	gr	1	5	17	A	733.38360	733.38348	2.00e−04
gr	3	4	17	A	gr	1	5	18	A	705.09980	705.09972	2.00e−04
gr	3	4	17	A	gr	2	3	16	A	596.12720	596.12718	2.00e−04
gr	3	4	17	A	gr	2	3	17	A	569.42750	569.42779	2.00e−04
gr	3	4	17	A	gr	3	5	16	A	228.40850	228.40828	2.00e−04
gr	3	4	17	A	gr	3	5	17	A	201.75370	201.75381	2.00e−04
gr	3	4	17	A^+	gr	3	5	18	A	173.53520	173.53518	2.00e−04
gr	3	4	18	A^+	gr	1	5	17	A	761.57069	761.57085	2.00e−04
gr	3	4	18	A^+	gr	1	5	18	A	733.28710	733.28709	2.00e−04
gr	3	4	18	A^+	gr	1	5	19	A	703.43697	703.43601	2.00e−04
gr	3	4	18	A^+	gr	2	3	17	A	597.61520	597.61516	2.00e−04
gr	3	4	18	A^+	gr	2	3	18	A	569.34906	569.34984	2.00e−04
gr	3	4	18	A^+	gr	3	5	17	A	229.94118	229.94118	2.00e−04
gr	3	4	18	A^+	gr	3	5	18	A	201.72259	201.72255	2.00e−04
gr	3	4	18	A^-	gr	3	5	19	A	171.94050	171.94061	2.00e−04
gr	3	4	18	A^-	gr	0	1	17	A^+	1015.66274	1015.66094	2.00e−04
gr	3	4	18	A^-	gr	0	1	18	A^-	1013.02252	1013.02352	2.00e−04
gr	3	4	18	A^-	gr	0	1	19	A^+	987.90040	87.90035	2.00e−04
gr	3	4	18	A^-	gr	1	5	17	A	261.569396	261.569384	2.00e−04
gr	3	4	18	A^-	gr	1	5	18	A	733.27992	733.27962	2.00e−04
gr	3	4	18	A^-	gr	1	5	19	A	703.42977	703.42987	2.00e−04
gr	3	4	18	A^-	gr	2	3	17	A	597.60812	597.60878	2.00e−04
gr	3	4	18	A^-	gr	2	3	18	A	569.34167	569.34193	2.00e−04
gr	3	4	18	A^-	gr	3	5	17	A	229.93361	229.93361	2.00e−04
gr	3	4	18	A^-	gr	3	5	18	A	201.71556	201.71596	2.00e−04
gr	3	4	18	A	gr	3	5	19	A	171.93375	171.93333	2.00e−04
gr	3	4	19	A	gr	1	5	18	A	763.03518	763.03539	2.00e−04
gr	3	4	19	A	gr	1	5	19	A	733.18610	733.18617	2.00e−04
gr	3	4	19	A	gr	1	5	20	A	701.71030	701.71009	2.00e−04
gr	3	4	19	A	gr	2	3	18	A	599.09709	599.09740	2.00e−04
gr	3	4	19	A	gr	2	3	19	A	569.26537	569.26592	2.00e−04
gr	3	4	19	A	gr	3	5	18	A	231.47190	231.47143	2.00e−04
gr	3	4	19	A	gr	3	5	19	A	201.68960	201.68964	2.00e−04
gr	3	4	19	A	gr	3	5	20	A	170.34500	170.34570	2.00e−04
gr	3	4	20	A	gr	1	5	20	A	733.08000	733.08090	2.00e−04
gr	3	4	20	A	gr	1	5	21	A	700.09903	700.09997	2.00e−04
gr	3	4	20	A	gr	2	3	19	A	600.57490	600.57409	2.00e−04
gr	3	4	20	A	gr	2	3	20	A	569.17659	569.17601	2.00e−04
gr	3	4	20	A	gr	3	5	19	A	232.99960	232.99986	2.00e−04
gr	3	4	20	A	gr	3	5	20	A	201.65450	201.65427	2.00e−04
gr	3	4	20	A	gr	3	5	21	A	160.74770	160.74747	2.00e−04

solved in our spectra so that our term values represent the centers of gravity of the hyperfine multiplets, which are split by only a few MHz at most.) The experimental term values were then fitted to power-series expansions of the form

$$E(v_t, K, J) = a_0 + a_1 J(J+1) + a_2 J^2(J+1)^2) + \cdots \quad (2)$$

in order to determine the J-independent torsion–K-rotation sub-state origin energies (coefficient a_0), effective B-values (coefficient a_1) and effective centrifugal distortion constants D (coefficient $-a_2$). A number of low-K sub-bands of A symmetry displayed resolved K-doublet asymmetry splittings which were fitted to the expression

$$\Delta(v_t, K, J) = [S + TJ(J+1) + UJ^2(J+1)^2 + \cdots] \times [(J+K)!/(J-K)!] \quad (3)$$

Wavenumbers calculated from the Taylor-series coefficients for the assigned lines generally agree with the observations for unblended lines to well within the estimated ±0.0002 cm^{-1} uncertainty, as shown for the majority of the sample transitions in Table 3. Here, we will not explicitly present tables of the Taylor-series expansion coefficients and K-doubling parameters obtained using Eqs. (2) and (3), but have included these along with our files of assigned line positions and Ritz term values for A and E species as Supplementary material.

While the Ritz program gives accurate relative energies for a family of states connected by transitions it does not determine the absolute energies since only energy differences are observable. Thus, the reference energy must be chosen individually for each separate family of states that is not connected to another family. With our extended assignments, we have now connected previously separate families from [4] so just have the two families remaining for the A and E symmetry species that are independent of each other. In the present work, we have chosen to fix the reference energies for the A and E species at the values calculated for the $(v_t, K) = (0, 0)$ levels from the customary one-dimensional torsional Hamiltonian using the previously reported molecular constants [4].

Table 4
Sample set of $CH_3{}^{17}OH$ ground-state term values determined by the Ritz program, with uncertainties ε and the number N of independent transitions connected to each level.

v	v_t	K	J	Sy	Ritz val. (cm^{-1})		N^a
gr	3	4	4	A	1170.265171	(92)	3
gr	3	4	5	A	1178.10408	(13)	6
gr	3	4	6	A	1187.510530	(93)	6
gr	3	4	7	A	1198.48418	(11)	7
gr	3	4	8	A	1211.02474	(10)	7
gr	3	4	9	A	1225.13191	(12)	7
gr	3	4	10	A	1240.805341	(85)	7
gr	3	4	11	A	1258.044694	(99)	7
gr	3	4	12	A	1276.84962	(20)	7
gr	3	4	13	A	1297.219468	(74)	7
gr	3	4	14	A	1319.154031	(83)	7
gr	3	4	15	A	1342.65250	(10)	7
gr	3	4	16	A	1367.714683	(51)	7
gr	3	4	17	A	1394.33949	(14)	8
gr	3	4	18	A^+	1422.52686	(11)	8
gr	3	4	18	A^-	1422.51964	(26)	11
gr	3	4	19	A	1452.27594	(12)	8
gr	3	4	20	A	1483.58552	(17)	7
gr	3	4	21	A	1516.45534	(12)	6
gr	3	4	22	A	1550.884677	(99)	5
gr	3	4	23	A	1586.87231	(17)	6
gr	3	4	24	A	1624.41782	(22)	4
gr	3	4	25	A	1663.520597	(67)	2
co	0	1	14	A^-	1323.442715	(10)	3
co	0	1	15	A^+	1343.79003	(28)	3
co	0	1	15	A^-	1347.0146545	(89)	3
co	0	1	16	A^+	1368.501210	(36)	3
co	0	1	16	A^-	1372.150761	(57)	3
co	0	1	17	A^+	1394.7514135	(98)	3
co	0	1	17	A^-	1398.850577	(38)	3
co	0	1	18	A^+	1422.54543	(17)	10
co	0	1	18	A^-	1427.11182	(13)	4
co	0	1	19	A^+	1451.861846	(16)	3
co	0	1	19	A^-	1456.933126	(59)	3
co	0	1	20	A^+	1482.72094	(11)	3
co	0	1	20	A^-	1488.31246	(19)	3
co	0	1	21	A^+	1515.114057	(17)	2
co	0	1	21	A^-	1521.248382	(68)	2
co	0	1	22	A^+	1549.043178	(58)	2
co	0	1	22	A^-	1555.73830	(32)	2
co	0	1	23	A^+	1584.497971	(63)	2
co	0	1	23	A^-	1591.780972	(88)	2

[a] Number of assigned lines starting from each level.

An important application for our term value dataset is the prediction of sub-millimetre transition frequencies for the astronomical community. As discussed in our earlier work [4], a good estimate of the accuracy of such predictions could be obtained by comparing combination differences from independent pairs of transitions, from which we determined the accuracy for a single unblended line to be of order 1 MHz. Thus, we believe that predictions from our data will be reliable to within a few MHz (neglecting the small quadrupole hyperfine shifts), approaching the value needed by the radio astronomers. In particular, the frequencies of $\Delta K = 0$ a-type lines can be predicted from combination differences among the transitions of a single sub-band. Since the a-type lines cluster in close multiplets across the submillimeter region and are one of the most prominent features of the methanol spectrum, their accurate prediction is particularly crucial for astronomical purposes. Thus, a database of a-type line positions for $CH_3{}^{17}OH$ will represent an important output from our study.

4. Fourier fit to CO-stretching τ-curves and Fermi resonances

As illustrated previously for several isotopologues of methanol [7–10], the curves of torsion–vibration energies as a function of K for the CO-stretching state are crossed at sharp angles by the curves for high $v_t = 3$ or $v_t = 4$ levels of the ground-state torsional manifold, resulting in K-localized anharmonic Fermi resonances. In particular, the $(\sigma\ v_t\ K)^v = (A^+\ 0\ 0)^{co}$ levels are perturbed downward by the $(A^+\ 4\ 0)^{gr}$ levels lying just above (interaction with the $v_t = 3\ 0A^+$ levels is forbidden) while the $(E\ 0\ -5)^{co}$ levels are also repelled downwards by the $(E\ 3\ -5)^{gr}$ levels just above. As shown in Fig. 5, the shifts are quite distinct in a plot of the CO-stretching sub-band origins from Tables 1 and 2, in which we have arranged the origins in "τ-curves" with the origins sorted by Dennison's index τ(=1, 2 or 3). This index is related to the torsional symmetry by the rule $(\tau + K) = 3N + 1$, $3N$ or $3N - 1$ for A, E $(K > 0)$ and E $(K < 0)$, respectively, where N is an integer [13]. It can be seen that both the $K = 0A$, $\tau = 1$ origin (which is almost degenerate with $K = 0E$, $\tau = 2$ or 3 and is almost hidden in Fig. 5) and the $K = -5E$, $\tau = 3$ origin are perturbed sharply downwards, while their neighbors are shifted slightly upwards.

In order to put the shifts on a more quantitative basis and obtain estimates of their magnitudes, we have explored a simple Fourier picture for the τ-curves. In Dennison's model [13], the torsional energies of given τ are oscillatory functions with period 3 in a variable $(1 - \rho)K$, with $\rho \approx I_{CH3}/I_a$, where I_{CH3} is the axial moment of inertia of the methyl top and I_a is that of the entire molecule. Thus, they can be expanded in Fourier series and the sub-band origins can conveniently be represented by a simple 5-parameter model of the form [14]

$$v_0(\tau, K) = c_0 + c_1 \cos\{[(1-\rho)K + \tau - 1]2\pi/3\} + c_2 \cos\{[(1 - \rho)K + \tau - 1]4\pi/3\} + \Delta[A - B]K^2 \quad (4)$$

where c_0, c_1 and c_2 are Fourier coefficients, $\Delta[A - B]$ is the change in the effective rotational parameter $[A - (B + C)/2]$ between excited and ground states, and no change is assumed in ρ. We fitted the sub-band origins to Eq. (4) using the Solver function in Microsoft Excel, excluding the five origins expected to be perturbed, and obtained the coefficients shown in Table 5. The origins calculated with these constants are shown as the lines in Fig. 5, and indicate that the simple model gives quite a good representation of the data. As a comparison, we also applied Eq. (4) with the Solver function directly to the substate origins obtained via Eq. (2) for the CO-stretching and $v_t = 0$ ground states separately. The results are included in Table 5 and the differences between the CO-stretching and ground-state values are seen to be reasonably consistent with the results of the sub-band fit, with some discrepancy in the value of ρ.

Since the Fourier fit seems to work quite well, we can take the differences between observed and calculated sub-band origins as reasonable estimates of the anharmonic Fermi shifts for the five states that were excluded from the fit. These shifts are listed in Table 6, together with the resonance denominators for the Fermi interactions determined as the differences between the $v_t = 0$ CO-stretching and $v_t = 3$ ground-state a_0 Taylor-series coefficients given in the Supplementary material. (The $v_t = 3$ and $v_t = 4$ substates are near-degenerate for the $K = 0A$ levels so we simply used the $v_t = 3$ value although the interaction is with $v_t = 4$.) By treating the resonances as simple 2×2 interactions with an off-diagonal coupling parameter H_{int}, we can then solve the secular determinants for the values of H_{int} and also the mixing ratio $|b/a|$ for the eigenfunction coefficients, which are listed in Table 6. Our values for the Fermi shifts are comparable to those found previously for other isotopologues, and indicate that the interaction parameters are quite sizeable.

5. Level-crossing resonances

There is also evidence in the spectrum for two other interactions involving J-dependent perturbations due to level crossings.

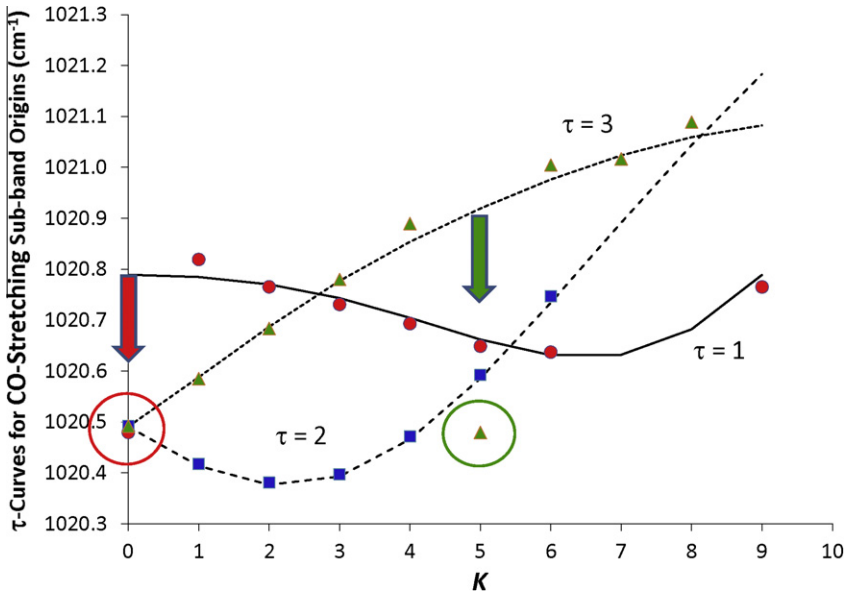

Fig. 5. τ-curves for origins of sub-bands of the CO-stretching fundamental of $CH_3{}^{17}OH$, highlighting the strong downward Fermi shifts of the $K = 0A$ $\tau = 1$ and $-5E$ $\tau = 3$ levels due to anharmonic coupling with ground-state $v_t = 4$ and $v_t = 3$ levels, respectively.

Table 5
Parameters from Fourier fits to CO-stretching sub-band origins and to substate origins for the CO-stretching and $v_t = 0$ ground vibrational states of $CH_3{}^{17}OH$.

Parameter	Sub-band origins	CO-stretch substates	Ground substates	CO–Gr difference
c_0 (cm^{-1})	1020.590	1154.299	133.736	1020.564
c_1 (cm^{-1})	0.2228	−5.9743	−6.1808	0.2065
c_2 (cm^{-1})	−0.0239	0.2131	0.2403	−0.0272
$[A - B]$ (cm^{-1})	0.00528[a]	3.46128	3.45465	0.00663
ρ	0.81562	0.80892	0.80957	

[a] This is the difference in effective $[A - B]$ constant between the $v_t = 0$ CO-stretching and ground states.

Table 6
Perturbation shifts δ, coupling matrix elements H_{int} and $|b/a|$ eigenfunction mixing ratios for Fermi anharmonic resonances between CO-stretching and $v_t = 3$ or $v_t = 4$ ground-state levels of $CH_3{}^{17}OH$.

K	τ	a	Shift δ[a]	ΔE(co–gr)	H_{int}	$\lvert b/a \rvert$
0	1	A	−0.3094	−22.496	2.64	0.1173
−1	1	E	0.0345	39.438	1.17	0.0296
4	3	A	0.0359	49.986	1.34	0.0268
−5	3	E	−0.4402			
6	3	E	0.0284	31.811	0.95	0.0299

[a] Shifts are taken as the differences between the c_0 sub-band origins and the Fourier fit calculated values. Units are cm^{-1} for δ, ΔE and H_{int}.

The first is a broad $\Delta K = 1$ Coriolis-type resonance between the $5E$ $v_t = 0$ CO-stretching and the $6E$ $v_t = 3$ ground-state levels. As determined from the a_0 Taylor-series coefficients, the $(\sigma, v_t, K)^v = (E, 0, 5)^{co}$ origin lies only 1.541 cm^{-1} above that of the $(E, 3, 6)^{gr}$ substate, so that this close accidental near-degeneracy leads to observable perturbation. In difference tables of the sub-branch wavenumbers for the $(E, 0, 5)^{co}$ sub-band, the second differences vary markedly with J, indicating a strong J-dependent interaction typical of $\Delta K = 1$ coupling. The effects are illustrated in Fig. 6, showing J-reduced term values for the coupled states obtained by subtracting a J-rotational energy of $0.78J(J + 1)$, where 0.78 cm^{-1} is a typical effective B-value, in order to get near-horizontal curves. Because the B-value is larger for the $v_t = 3$ ground state than the excited CO-stretching state, the $(E, 3, 6)^{gr}$ levels rise towards the $(E, 0, 5)^{co}$ levels and then start to repel them upwards in a broad avoided-crossing resonance as the near-degeneracy gets closer at high J. Unfortunately we are not currently able to follow the $(E, 3, 6)^{gr}$ sub-band in the FIR spectrum through the crossing region of strong perturbation, so do not have the energy separations needed to model the interaction and obtain the coupling constant.

The second resonance is a highly localized $\Delta K = 3$ interaction due to a near degeneracy between the $(A^+, 0, 1)^{co}$ and $(A^-, 3, 4)^{gr}$ substates at $J = 18$, mentioned previously in connection with Fig. 1 and Table 3 and clearly evident from the term values given in Table 4. The energy level picture as a function of J is shown in Fig. 7, with the energies normalized with respect to the $(A^+, 0, 0)^{co}$ levels taken as zero. Due to the large asymmetry splitting of the $(A^{\pm}, 0, 1)^{co}$ K-doublet levels, the curve for the A^+ component slopes downward and meets the rising curve for the $(A^{\pm}, 3, 4)^{gr}$ doublet levels at a relatively sharp angle, producing a very close degeneracy just at $J = 18$. Since the selection rule for $\Delta J = 0$ coupling with odd Δv_t is $A^+ \leftrightarrow A^-$, only the A^- component of the $4A$ doublet is affected and is perturbed downward at $J = 18$, producing an observable splitting of the $4A$ doublet at that point. In Fig. 1, the $Q(18)$ A^+ component of the $(v_t, K) = (3, 4) \leftarrow (3, 5)A$ sub-band is seen to be unshifted in the Q-branch J-sequence while the A^- component is split off to lower wavenumber. Conversely, in the CO-stretching state, the $1A^+$ $v_t = 0$ level is perturbed upwards at $J = 18$, creating a small but distinct irregularity in the wavenumber second differences for the $1A^+$ sub-band.

This interaction has also been seen previously for the normal [15,16] and C-13 [9] methanol species but not for the O-18 isotopologue [10], giving a nice example of the effects of isotopic tuning of the resonances. The $v_t = 3$ ground-state energies do not change greatly with isotopic substitution, whereas the CO-stretching band origin shifts downwards from about 1033 to 1021 to 1018 to 1007 cm^{-1} in going from the normal species to O-17 to C-13 and then to O-18. If one looks at Fig. 7 and mentally shifts the CO-stretching curves up by about 10 cm^{-1} relative to the $v_t = 3$ ground-state curves (thus corresponding to Fig. 3 of [15]), one sees that the $(A^{\pm}, 3, 4)^{gr}$ curve will now cross both the $(A^+, 0, 0)^{co}$ and $(A^+, 0, 1)^{co}$ curves at around $J = 27$ and $J = 35$, respectively, just as

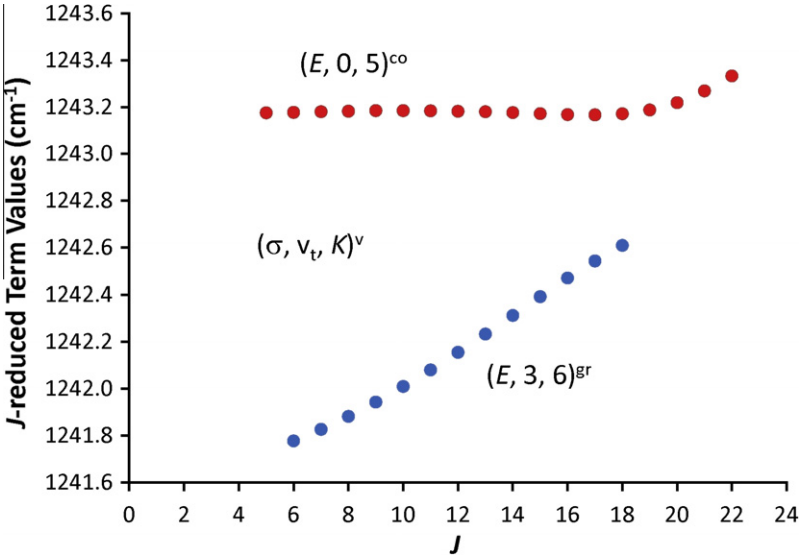

Fig. 6. J-reduced term values for the near-degenerate $(\sigma, v_t, K)^v = (E, 0, 5)^{co}$ and $(E, 3, 6)^{gr}$ substates of $CH_3{}^{17}OH$, illustrating the onset of strong perturbation at higher J with a broad avoided crossing resonance.

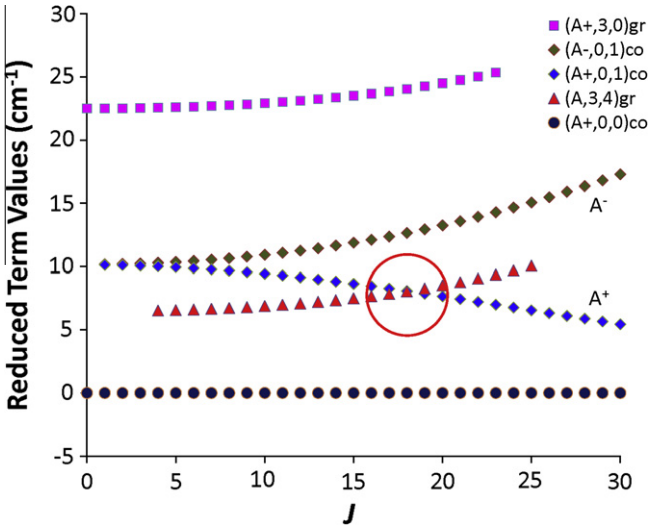

Fig. 7. Localized level-crossing resonance between the $(\sigma, v_t, K)^v = (A^+, 0, 1)^{co}$ and $(A^-, 3, 4)^{gr}$ substates of $CH_3{}^{17}OH$ at $J = 18$. The term values are normalized relative to those of the $(A^+, 0, 0)^{co}$ substate, taken as zero.

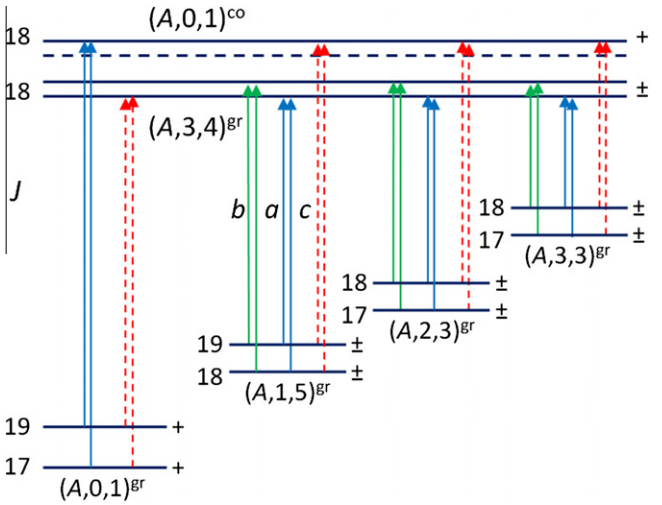

Fig. 8a. Schematic energy level and transition diagram (not to scale) for the level-crossing resonance between the $J = 18$ levels of the $(\sigma, v_t, K)^v = (A^+, 0, 1)^{co}$ and $(A^-, 3, 4)^{gr}$ substates of $CH_3{}^{17}OH$, showing the splitting of the $(A, 3, 4)^{gr}$ K-doublet due to the perturbation and the presence of forbidden transitions (dashed lines) due to mixing of the interacting levels and consequent intensity borrowing. Close triplets of lines appear in the spectrum originating from each of the six lower levels on the right of the diagram.

is observed for the normal species [15,16]. On the other hand, if one shifts the CO-stretch curves down by about 3 cm^{-1} so that the $(A^{\pm}, 3, 4)^{gr}$ curve starts out just above the $(A^-, 0, 1)^{co}$ curve, then a very broad avoided crossing results, exactly as seen for the C-13 species [9]. Lastly, if one lowers the CO-stretch curves by 14 cm^{-1} in going to the O-18 species, then the $(A^{\pm}, 3, 4)^{gr}$ resonances are completely detuned and instead it is now the $(A^+, 3, 0)^{gr}$ levels that then come into coincidence with higher $(A^{\pm}, 0, 3)^{co}$ levels of the CO-stretching state [10].

The spectral data completely characterize the resonance in Fig. 7, as is illustrated schematically in Fig. 8a, and permit a quantitative 2×2 analysis of the coupling. For the $J = 18$ $(A^-, 3, 4)^{gr}$ level, the magnitude δ of the perturbation is given directly by the observed doublet splitting for $P(19)$, $Q(18)$ or $R(17)$ line pairs in the $(v_t, K) = (3, 4) \leftarrow (3, 5)$, $(3, 4) \leftarrow (2, 3)$ and $(3, 4) \leftarrow (1, 5)$ FIR sub-bands, while for the $(A^+, 0, 1)^{co}$ levels, estimates of the perturbation are also provided by the residuals in the power-series fit for the $1A^+$ CO-stretching sub-band with the perturbed lines weighted to zero. As can be determined from the listing in Table 3, our six independent strong FIR transition doublets give an average shift of $\delta = 0.00714$ cm^{-1}. Next, since the perturbation mixes the $J = 18$ $(A^+, 0, 1)^{co}$ and $(A^-, 3, 4)^{gr}$ levels, forbidden transitions become visible in the spectrum through intensity borrowing, and the separation ΔE between the perturbed levels is given by the frequency difference between allowed and forbidden transitions from a common lower level. Here we have eight pairs of transitions giving an average separation of $\Delta E = 0.02584$ cm^{-1}. With the unperturbed separation ΔE_o equal to $(\Delta E - 2\delta)$, the solution of the 2×2 secular determinant gives the interaction matrix element H_{int} and the mixing ratio $|b/a|$ of the coefficients of the mixed eigenfunctions as

Table 7
Perturbation shifts $\delta(J)$, coupling matrix elements H_{int} and $|b/a|$ eigenfunction mixing ratios for J-localized level-crossing resonance between $(\sigma, v_t, K)^v = (A^+, 0, 1)^{co}$ and $(A^-, 3, 4)^{gr}$ levels of $CH_3{}^{17}OH$.

J	$\delta(J)$[a]	$\Delta E(J)$	$\Delta E_o(J)$	H_{int}	$\lvert b/a\rvert$
17	0.00025	0.41194	0.41144	0.0101	0.0246
18	0.00670	0.02500	0.01160	0.0111	0.6051
19	−0.00045	−0.41406	−0.41316	0.0136	0.0330

[a] Shift of the $(A^+, 0, 1)^{co}$ level. The $(A^-, 3, 4)^{gr}$ shift is assumed to be equal and opposite. Units are cm^{-1} for δ, ΔE and H_{int}.

$$H_{int} = 0.5(\Delta E^2 - \Delta E_o^2)^{1/2} \quad (5)$$

$$|b/a| = [\delta/(\Delta E - \delta)]^{1/2} \quad (6)$$

The various parameters characterizing the interaction for $J = 17$–19 are listed in Table 7, showing that the degeneracy is extremely close with an unperturbed separation of only 0.01156 cm^{-1} at $J = 18$. The value of 0.62 for $|b/a|$ for $J = 18$ shows that the interacting levels are highly mixed and almost 40% of the original intensity of the allowed transitions will be borrowed by the forbidden partners. This is nicely illustrated in Fig. 8b showing the triplet of $P(19)$ lines originating from the $(A, 1, 5)^{gr}$ lower level.

6. Determination of molecular parameters

In order to characterize the positions of the origins of the ground-state FIR sub-bands, we fitted our A and E data with a basic RAM torsion–K-rotation Hamiltonian with the addition of one sextic term. Table 8 lists the parameters included, along with their matrix elements written in the explicit $(P_\gamma + \rho K)$ RAM form of the torsional angular momentum, where P_γ represents the angular momentum of the methyl top. As before [4], we constrained the k_6 parameter to zero to remove the known linear dependence in the non-reduced Hamiltonian and we again found that k_1 and k_7 were essentially undetermined. In the least squares fits, the origins were weighted by the inverse squares of their standard deviations from the Taylor-series fits, as given in parentheses in Tables 1 and 2. The (obs.–calc.) residuals for the A and E sub-band origins are listed in the last columns of Tables 1 and 2. They show that the sub-band structure is reasonably well modeled over all torsional states from $v_t = 0$ to $v_t = 3$ for a wide range of K with an overall unweighted rms deviation σ of 0.042 cm^{-1} given in Table 8. However, the value of χ^2 for the fit was 1855, showing that we still have a long way to go to achieve experimental accuracy and that more complete global modeling will undoubtedly be needed in future.

Table 8
Parameters for the ground vibrational state of $CH_3{}^{17}OH$ from a least-square fit to a basic torsion–K-rotation model for the substate origins.

Parameter	Matrix element	Value (cm^{-1})	
C_k	K^2	3.45835	(79)
F	$\langle(\hat{P}_\gamma + \rho K)^2\rangle$	27.5284	(11)
ρ		0.8092749	(70)
V_3	$\langle 1 - cos3\gamma\rangle/2$	373.845	(18)
V_6	$\langle 1 - cos6\gamma\rangle/2$	−1.299	(20)
D_k	$-K^4$	2.6	$(12) \times 10^{-05}$
Φ_k	K^6	−5.9	$(53) \times 10^{-08}$
k_1	$K^3\langle\hat{P}_\gamma + \rho K\rangle$	0.0	(Fixed)
k_2	$K^2\langle(\hat{P}_\gamma + \rho K)^2\rangle$	−1.813	$(12) \times 10^{-03}$
k_3	$K\langle(\hat{P}_\gamma + \rho K)^3\rangle$	−5.077	$(21) \times 10^{-03}$
k_4	$\langle(\hat{P}_\gamma + \rho K)^4\rangle$	−8.545	$(31) \times 10^{-03}$
k_5	$K^2\langle 1 - cos3\gamma\rangle$	1.045	$(17) \times 10^{-02}$
k_6	$K\langle(\hat{P}_\gamma + \rho K)(1 - cos3\gamma)\rangle$	0.0	(Fixed)
k_7	$\langle(\hat{P}_\gamma + \rho K)^2(1 - cos3\gamma)\rangle$	0.0	(Fixed)
σ		0.04214	

For the excited CO-stretching state, Table 5 provides a value of 1020.564 cm^{-1} for the band origin. The B value deduced from the a_1 parameters of Tables 1 and 2 is 0.7806 cm^{-1} for the CO stretch compared to 0.7892 cm^{-1} for the ground state. This difference is consistent with the value of about −0.017 cm^{-1} seen consistently for the low-J second differences between the CO-stretching sub-band wavenumbers, which is equal to $2(B' - B'')$ in lowest order. The value of $[A - B]$ increases for the CO stretch by approximately 0.006 cm^{-1} as seen from Table 5. More detailed modeling of the CO-stretching state really requires more extensive information on excited torsional CO-stretching levels, which we hope to obtain in future with further assignment work.

7. Conclusions

In this study we have investigated the far-infrared and CO-stretching synchrotron Fourier transform spectra of $CH_3{}^{17}OH$ recorded at the far-infrared beamline of the Canadian Light Source. Using the Ritz program, we were able to extend knowledge of the ground vibrational state to 123 new torsion–rotation sub-bands at higher torsional and K-rotational quantum number, with energy term values now determined for levels with quantum numbers in the ranges $v_t \leqslant 3$, $J \leqslant 30$ and $|K| \leqslant 12$. The term values and sub-bands were fitted to Taylor-series expansions in powers of $J(J + 1)$ in order to obtain their J-independent origins. Files of the

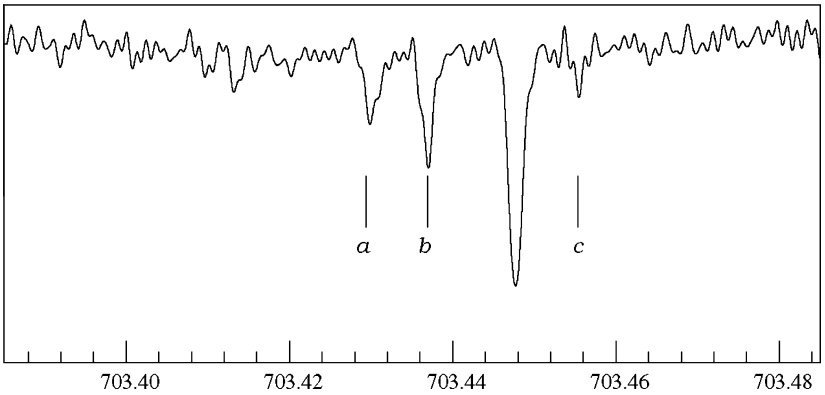

Fig. 8b. Spectral trace showing the triplet of lines for transitions labeled as a, b and c in the energy level diagram in (a). Line wavenumbers are a = 703.42977, b = 703.43697 and c = 703.45547 cm^{-1}.

assigned line positions, Ritz term values and Taylor coefficients have been included as Supplementary material. Mapping of the CO-stretching sub-band origins against K and fitting with a simple Fourier model allowed determination of Fermi shifts for five sub-states due to K-localized anharmonic Fermi perturbations and the calculation of approximate coupling constants. Two Coriolis level-crossing resonances have also been observed involving coupling between CO-stretching and $v_t = 3$ ground state levels. The FIR sub-band origins were fitted to a low-order torsion–rotation Hamiltonian in order to obtain ground-state torsion–K-rotation molecular parameters characterizing the ground-state energy manifold.

Acknowledgements

A. Predoi-Cross and R.M. Lees acknowledge financial support from the Natural Sciences and Engineering Research Council of Canada. The research described in this paper was performed at the Canadian Light Source, which is supported by NSERC, NRC, CIHR, and the University of Saskatchewan. We are pleased to join in celebrating the many achievements of our friends and colleagues, Bob McKellar and Phil Bunker, and look forward to further fruitful interaction and collaboration in the future.

Appendix A. Supplementary material

For articles with electronic supplementary data, add the following as an Appendix to the article: Supplementary data for this article are available on ScienceDirect (www.sciencedirect.com) and as part of the Ohio State University Molecular Spectroscopy Archives (http://library.osu.edu/sites/msa/jmsa_hp.htm). Also follow style instructions from previous Word version of style sheet.

Supplementary data associated with this article can be found, in the online version, at doi:10.1016/j.jms.2011.05.007.

References

[1] Final Report, Workshop on Laboratory Spectroscopy in Support of Herschel, SOFIA and ALMA, Pasadena, CA, 2006, <www.submm.caltech.edu/labspec>.
[2] Y. Hoshino, M. Ohishi, K. Takagi, J. Mol. Spectrosc. 148 (1991) 506.
[3] L.-H. Xu, P.M. Bance, R.M. Lees, C. Styger, M.C.L. Gerry, in: M.N. Afsar (Ed.), Int. Conf. on Millimeter and Submillimeter Waves and Applications, San Diego, CA, Proc. SPIE 2250, 1994, pp. 94–95.
[4] G. Moruzzi, R.J. Murphy, R.M. Lees, A. Predoi-Cross, B.E. Billinghurst, Mol. Phys. 108 (2009) 2343–2353.
[5] G. Moruzzi, L.-H. Xu, R.M. Lees, B.P. Winnewisser, M. Winnewisser, J. Mol. Spectrosc. 167 (1994) 156–175.
[6] N. Ioli, G. Moruzzi, et al., J. Mol. Spectrosc. 171 (1995) 130.
[7] G. Moruzzi, B.P. Winnewisser, M. Winnewisser, I. Mukhopadhyay, F. Strumia, Microwave, Infrared, and Laser Transitions of Methanol, Atlas of Assigned Lines from 0 to 1250 cm^{-1}, CRC Press, Boca Raton, FL, 1995.
[8] W.H. Weber, P.D. Maker, J. Mol. Spectrosc. 93 (1982) 131–153.
[9] I. Mukhopadhyay, R.M. Lees, W. Lewis-Bevan, J.W.C. Johns, J. Chem. Phys. 102 (1995) 6444–6455.
[10] R.M. Lees, R.J. Murphy, G. Moruzzi, A. Predoi-Cross, Li-Hong Xu, D.R.T. Appadoo, B. Billinghurst, R.R.J. Goulding, S.B. Zhao, J. Mol. Spectrosc. 256 (2009) 91–98.
[11] A. Ibrahim, A. Predoi-Cross, P.M. Teillet, Techniques for handling and removal of spectral channels in Fourier transform synchrotron based spectra, in: Proceedings of the 5th International Workshop on Infrared Microscopy and Spectroscopy with Accelerator Based Sources, AIP 1214, 2009, pp. 97–99.
[12] J. Fisher, G. Paciga, Li-Hong Xu, S.B. Zhao, G. Moruzzi, R.M. Lees, J. Mol. Spectrosc. 245 (2007) 7–20.
[13] J.S. Koehler, D.M. Dennison, Phys. Rev. 57 (1940) 1006–1021.
[14] R.M. Lees, M. Mollabashi, Li-Hong Xu, M. Lock, B.P. Winnewisser, Phys. Rev. A 65 (2002) 042511.
[15] J.C. Pearson, C.S. Brauer, B.J. Drouin, Li-Hong Xu, Can. J. Phys. 87 (2009) 449–467.
[16] R.M. Lees, Li-Hong Xu, J.W.C. Johns, B.P. Winnewisser, M. Lock, J. Mol. Spectrosc. 243 (2007) 168–181.